Proc. Natl. Acad. Sci. USA
Vol. 87, pp. 7200–7204, September 1990
Biophysics

Global processing of visual stimuli in a neural network of coupled oscillators

(orientation tuning/parallel computation/primary visual cortex/statistical mechanics/temporal coherence)

H. SOMPOLINSKY*†, D. GOLOMB‡, AND D. KLEINFELD*

*AT&T Bell Laboratories, Murray Hill, NJ 07974; and ‡Racah Institute of Physics, Hebrew University, Jerusalem, Israel 91904

Communicated by Pierre C. Hohenberg, June 12, 1990 (received for review April 10, 1990)

ABSTRACT **An oscillator neural network model is presented that is capable of processing local and global attributes of sensory input. Local features in the input are encoded in the average firing rate of the neurons while the relationships between these features can modulate the temporal structure of the neuronal output. Neurons that share the same receptive field interact via relatively strong feedback connections, while neurons with different fields interact via specific, relatively weak connections. This pattern of connectivity mimics that of primary visual cortex. The model is studied in the context of processing visual stimuli that are coded for orientation. We compare our theoretical results with recent experimental evidence on coherent oscillatory activity in the cat visual cortex. The computational capabilities of the model for performing discrimination and segmentation tasks are demonstrated.**

The linking of sensory inputs across multiple sensory receptive fields is a fundamental task of sensory processing (1–3). Such linkage is necessary to identify distinct objects, segment them from each other, and separate them from background. The theoretical issues raised by this processing have been difficult to approach within the framework of most current neural network models. This difficulty originates from using only the levels of activity in individual neurons to encode information. It has been suggested by von der Malsburg and Schneider (1) that global properties of stimuli are identified through correlations in the temporal firing patterns of different neurons. This concept has gained support from a recent series of experiments by Eckhorn *et al.* (4) and by Singer and colleagues (5–7), who have shown that neurons in the cat primary visual cortex can exhibit oscillatory responses that are coherent over relatively large distances and are sensitive to global properties of stimuli.

In the present work we construct a model neural network that is capable of linking activity in disparate visual receptive fields in a manner that depends on extended features of the stimulus. The network is comprised of neurons that act as oscillators. The amplitude of their output corresponds to the average neuronal firing rate and the phase describes the temporal structure of the neuronal outputs.

In this study we focus on specifying the pattern of connectivity that is capable of generating spatial and temporal coherence in neuronal output similar to that observed in experiments. The model incorporates three aspects of the architecture of primary visual cortex: (*i*) The average firing rate of neurons is a strong function of the orientation of a moving bar or grating that passes through the receptive field of the cell (8). (*ii*) Nearby neurons have overlapping receptive fields and appear to be highly interconnected (9). (*iii*) Neurons with nonoverlapping receptive fields form a sparse set of long-range connections whose pattern appears to depend on the orientation preferences of the pre- and postsynaptic cell (9).

Before describing the model, we summarize the current status of experimental results that are relevant to our work. (*i*) Neurons that respond to moving, oriented bars have a periodic component in their spiking output. The average period, ≈20–30 ms, appears to be the same for different neurons and is independent of the orientation of the stimulus (4, 5). (*ii*) The activity of neurons that share a receptive field can be synchronized by the presentation of a single, oriented bar. The synchronization is fairly insensitive to the orientation preferences of the neurons (4–7). (*iii*) Neurons with separate receptive fields will fire in synchrony *only* if bars that simultaneously pass through the individual fields have similar orientation (6, 7). Interestingly, this occurs even though the coherent activity of neurons that share the same receptive field is largely independent of the orientation of the stimulus. (*iv*) The strength of the synchronization of the activity of neurons with different receptive fields is significantly enhanced by the use of a single long bar that extends across several fields, rather than two discontinuous, short bars (6). (*v*) The outputs of neurons with different receptive fields are not synchronized if the two stimuli move in opposite directions, even for neurons that respond vigorously to both directions of motion (6, 7). (*vi*) There were no substantial phase shifts in the temporal coherence for any of the experimental paradigms (4–7).

MODEL

Phase Equations. The firing of the neurons is considered as a stochastic event, described by the probability per unit time that the neuron at location $\mathbf{r}$ will fire at time t. This probability function, $P(\mathbf{r}, t)$, is assumed to have the form

$$P(\mathbf{r}, t) = V(\mathbf{r})\,(1 + \lambda \cos \Phi(\mathbf{r}, t)). \qquad [1]$$

The phases $\Phi(\mathbf{r}, t)$ parametrize the temporal firing pattern of the neurons. The coefficient λ corresponds to the relative contribution of the temporally modulated neuronal activity. The amplitude $V(\mathbf{r})$ is the normalized firing rate *averaged* over the duration of stimulus. If no stimulus is present within the receptive field of the neuron at $\mathbf{r}$, $V(\mathbf{r}) = 0$. With a stimulus moving across the field, $V(\mathbf{r})$ is taken to coincide with the "tuning" curve of the neuron; i.e., $V(\mathbf{r}) = V(\theta_0(\mathbf{r}) - \theta(\mathbf{r}))$, where $\theta_0(\mathbf{r})$ is the orientation of the stimulus and $\theta(\mathbf{r})$ is the orientation preferred by the neuron (Fig. 1*A*). Stimuli move along an axis that is perpendicular to their orientation. The difference in response to forward and reverse movement on this axis is the difference between $V(\theta)$ and $V(\theta - 180°)$.

The phase variables that govern the temporal aspects of the neuronal activity are assumed to obey equations for a system

The publication costs of this article were defrayed in part by page charge payment. This article must therefore be hereby marked "*advertisement*" in accordance with 18 U.S.C. §1734 solely to indicate this fact.

†On leave from Racah Institute of Physics, Hebrew University, Jerusalem, Israel 91904.

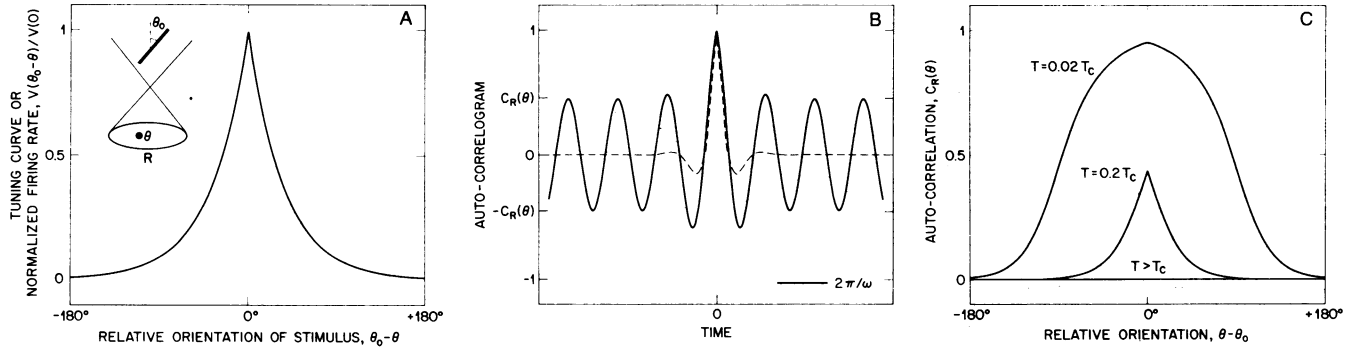

FIG. 1. Properties of individual neurons. The neuron in the **R**th cluster has orientation preference θ and is stimulated by a moving bar with orientation θ_0. (*A*) Tuning curve assumed for the neuron, described by $V(x) = e^{-|x|/\sigma}$ with $\sigma = 36°$ (8). (*B*) Time-dependent part of the autocorrelogram calculated (see *Appendix* and the text) for a neuron that is stimulated at its preferred orientation; i.e., $\theta = \theta_0$. We chose $W_S = 0.2$, for which $\tau_S \simeq 3\tau_0$ (the text) and $T_C = 0.1$ (*Appendix*), with $T = 0.2T_C$ (solid line) and $T = 5T_C$ (dashed line). The period of oscillations was taken as $2\pi/\omega = 8\ \tau_0$. (*C*) Dependence of the long-time limit of the autocorrelation function on the orientation of the stimulus relative to the preferred orientation of the neuron.

of coupled phase oscillators with noise (10); i.e.,

$$\tau_0\dot{\Phi}(\mathbf{r}, t) = \omega\tau_0 + \eta(\mathbf{r}, t) - \sum_{\mathbf{r}'\neq\mathbf{r}} J(\mathbf{r}, \mathbf{r}')\sin(\Phi(\mathbf{r}, t) - \Phi(\mathbf{r}', t)), \quad [2]$$

where τ_0 is the neuronal time scale and ω is the frequency of the neuronal oscillations. We assume that $\tau_0 << 2\pi/\omega$; this is consistent with the estimates $\tau_0 \simeq 3$ ms and $2\pi/\omega \simeq 25$ ms from experiment (4, 5). The term $\eta(\mathbf{r}, t)$ represents white noise with variance $\langle\eta(\mathbf{r}, t)\eta(\mathbf{r}', t')\rangle = 2T\tau_0\delta_{\mathbf{r}\mathbf{r}'}\delta(t - t')$, where T is a measure of the noise level. The noise represents fluctuations in the input to a cell. The connection strength $J(\mathbf{r}, \mathbf{r}')$ mediates the interaction between the phases of the neurons at locations $\mathbf{r}$ and $\mathbf{r}'$. Lastly, the sum over $\mathbf{r}'$ includes all neurons in the network.

Architecture of the Connections. The interactions between the neuronal phases are assumed to encode information about the position and orientation of the stimulus. We postulate that they depend on the average level of activity of the pre- and postsynaptic cell; i.e.,

$$J(\mathbf{r}, \mathbf{r}') = V(\mathbf{r})W(\mathbf{r}, \mathbf{r}')V(\mathbf{r}'), \quad [3]$$

where $W(\mathbf{r}, \mathbf{r}')$ specifies the architecture of the connections and is independent of the external stimulus.

A central element in this model is the introduction of short-range interactions that couple neurons with strongly overlapping receptive fields and long-range interactions that couple neurons with nonoverlapping receptive fields. We assume an architecture in which neurons are grouped into clusters, analogous to hypercolumns in the primary visual cortex (8). The neurons in each cluster respond to a stimulus in a common receptive field. They are labeled by the spatial coordinates of the cluster, denoted **R**, and their preferred orientation, θ, which is assumed to be uniformly distributed within each cluster.

Each neuron interacts with cells in the same cluster via short-range connections, taken as

$$W_{\mathbf{R}\mathbf{R}}(\theta, \theta') = W_S/N, \quad [4]$$

where N is the total number of neurons in the cluster that are activated by the stimulus. This form allows the coherence between two active neurons with the same receptive field to vary only moderately as a function of their preferred orientations. Neurons in different clusters interact via long-range connections, taken as

$$W_{\mathbf{R}\mathbf{R}'}(\theta, \theta') = W_L F(\theta - \theta')/N^2; \ \mathbf{R} \neq \mathbf{R}'. \quad [5]$$

We have assumed that $W_{\mathbf{R}\mathbf{R}'}(\theta, \theta')$ does not depend on the spatial separation between the clusters. The function $F(\theta - \theta')$ will be chosen, as described below, so that the phase coherence between different clusters will have a substantial dependence on the orientations of the stimuli. The relative strength of the long-range to the short-range connections scales as $1/N << 1$. This ensures that the coherence between neurons that share the same receptive field is largely independent of the *global* properties of the stimulus. The equations for the phase of each neuron (Eq. **2**), with the connection strengths defined by Eqs. **3–5**, constitute the model.

Correlation Functions. Coherent output in a population of neurons is deduced in experiment from the autocorrelogram of the output of each neuron and cross-correlograms of the output of pairs of neurons (4, 5). The correlograms can be expressed in terms of the correlation functions of the underlying phase variables in the model. We define

$$\Phi_{\mathbf{R}}(\theta, t) = \omega t + \phi_{\mathbf{R}}(\theta, t), \quad [6]$$

where $\phi_{\mathbf{R}}(\theta, t)$ represents the noisy component of the total phase $\Phi_{\mathbf{R}}(\theta, t)$ for a neuron in the **R**th cluster with orientation preference θ. The autocorrelogram is

$$\langle P_{\mathbf{R}}(\theta, t)P_{\mathbf{R}}(\theta, t + \tau)\rangle_t = V_{\mathbf{R}}^2(\theta)(1 + (\lambda^2/2)C_{\mathbf{R}}(\theta, \tau)\cos\omega\tau), \quad [7]$$

where $\langle\cdots\rangle_t$ denotes averaging over time ($t >> 1/\omega$), $V_{\mathbf{R}}(\theta) \equiv V(\theta_0(\mathbf{R}) - \theta(\mathbf{R}))$, and the autocorrelation function $C_{\mathbf{R}}(\theta, \tau) \equiv \langle\cos(\phi_{\mathbf{R}}(\theta, t) - \phi_{\mathbf{R}}(\theta, t + \tau))\rangle_t$ measures the temporal fluctuations in the phase. The cross-correlogram of the activity of a neuron in the **R**th cluster with orientation preference θ with one in the **R**'th cluster with orientation preference θ' is

$$\langle P_{\mathbf{R}}(\theta, t)P_{\mathbf{R}'}(\theta', t + \tau)\rangle_t = V_{\mathbf{R}}(\theta)V_{\mathbf{R}'}(\theta')(1 + (\lambda^2/2)C_{\mathbf{R}\mathbf{R}'}(\theta, \theta', \tau)\cos(\omega\tau + \chi)), \quad [8]$$

where the cross-correlation function $C_{\mathbf{R}\mathbf{R}'}(\theta, \theta', \tau) = \sqrt{a^2 + b^2}$ measures the amplitude of the phase coherence and $\chi = \chi_{\mathbf{R}\mathbf{R}'}(\theta, \theta', \tau) = \tan^{-1}(a/b)$ represents the average phase shift with $a \equiv \langle\sin(\phi_{\mathbf{R}}(\theta, t) - \phi_{\mathbf{R}'}(\theta', t + \tau))\rangle_t$ and $b \equiv \langle\cos(\phi_{\mathbf{R}}(\theta, t) - \phi_{\mathbf{R}'}(\theta', t + \tau))\rangle_t$.

RESULTS AND EXAMPLES

The model was analyzed using mean-field theory (see *Appendix*) and applies when the number of active neurons in each cluster is large ($N >> 1$). For concreteness, we assumed

that the tuning curve for every neuron has the shape shown in Fig. 1*A*. The main results are given below.

Temporal Coherence Within a Single Cluster. The presence of coherent oscillations depends on the rate of decay of the correlation functions. When the level of noise is large, the neurons behave as overdamped oscillators and both $C_{\mathbf{R}}(\theta, \tau)$ and $C_{\mathbf{RR}}(\theta, \theta', \tau)$ decay to zero in a time $\approx \tau_0/T << 1/\omega$ (Fig. 1*B*, dashed line). In contrast, the neurons exhibit persistent, coherent oscillations when the level of noise is below a critical value, T_C, where $T_C \propto W_S$. For noise levels less than T_C, the autocorrelation function decays from its initial value $C_{\mathbf{R}}(\theta, 0) = 1$ to a long-time limit $C_{\mathbf{R}}(\theta) \equiv \lim_{\tau\to\infty} C_{\mathbf{R}}(\theta, \tau) > 0$ (Fig. 1*B*, solid line). This rapid decay is characterized by a time-constant

$$\tau_S \simeq \tau_0/(2V_{\mathbf{R}}(\theta)W_S) \qquad [9]$$

and results in a peak in the autocorrelation function that is centered at $\tau = 0$ and has a width of $\approx 2\tau_S$. The magnitude of $C_{\mathbf{R}}(\theta)$ depends on θ as well as the level of noise (Fig. 1*C*). The presence of noise and the restricted number of active neurons in the cluster lead to an eventual decay of the correlation functions, characterized by a time-constant $\tau_L \approx N\tau_0/T >> 1/\omega$. Thus the long-time limit referred to above corresponds to $\tau_S << \tau << \tau_L$.

The cross-correlation functions between neurons in the same cluster do not have a substantial peak centered at $\tau = 0$. Their magnitude is related to the long-time limit of their autocorrelation functions through

$$C_{\mathbf{RR}}(\theta, \theta', \tau) = \sqrt{C_{\mathbf{R}}(\theta)C_{\mathbf{R}}(\theta')}. \qquad [10]$$

There are no phase shifts associated with the cross-correlation; i.e., $\chi = 0$ (Eq. **8**), as the short-range connections are excitatory. Thus, all of the active neurons in a cluster will fire coherently as a result of the extensive, short-range connectivity.

Temporal Coherence of Spatially Separated Clusters. The coherence between neurons that belong to two separate clusters depends on the coherence of the *average* phases of the clusters. The cross-correlation function between a neuron in the **R**th cluster with one in the **R**'th cluster is

$$C_{\mathbf{RR}'}(\theta, \theta', \tau) = \sqrt{C_{\mathbf{R}}(\theta)C_{\mathbf{R}'}(\theta')}\, C_{\mathbf{RR}'}, \qquad [11]$$

where $C_{\mathbf{RR}'}$ measures the correlation of the average phases of the two clusters for times $\tau << N\tau_0 \approx \tau_L$.

The value of $C_{\mathbf{RR}'}$ depends on the strength of the effective interaction between a cluster at **R** and one at **R**' and on the effective noise that tends to randomize the relative phases of the two clusters. The effective interaction, denoted $J_{\mathbf{RR}'}$, is a weighted average over the long-range connections $W_{\mathbf{RR}'}(\theta, \theta')$ between neurons in cluster **R** and those in **R**'; i.e.,

$$J_{\mathbf{RR}'} = \frac{W_L}{N} \times \int_0^{2\pi}\!\!\int \frac{d\theta d\theta'}{\sigma^2} V_{\mathbf{R}}(\theta)\sqrt{C_{\mathbf{R}}(\theta)}F(\theta - \theta')V_{\mathbf{R}'}(\theta')\sqrt{C_{\mathbf{R}'}(\theta')}, \qquad [12]$$

where σ is the width of the tuning curve (Fig. 1*A*). The effective interaction of $J_{\mathbf{RR}'}$ is a function of the difference in the orientation of the stimuli, $\Delta\theta_0 \equiv \theta_0(\mathbf{R}) - \theta_0'(\mathbf{R}')$. The magnitude of the effective noise that acts on the average phases of the clusters is T/N. Thus the ratio of the effective interaction strength to the effective noise level, which determines the magnitude of $C_{\mathbf{RR}'}$, is $W_L/T \approx 1$.

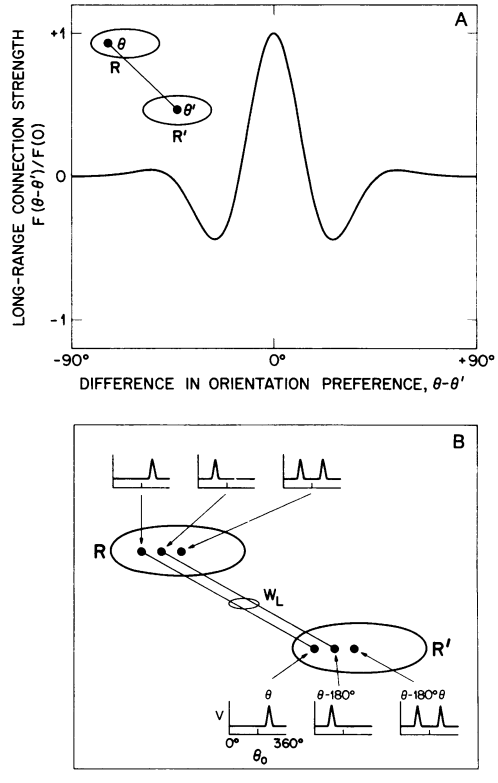

FIG. 2. Interaction between two spatially separated clusters. (*A*) Form of the long-range connectivity between neurons in different clusters with orientation preferences θ and θ', respectively; $F(x) = (1 - \sigma^2\partial^2/\partial x^2)^2 e^{-x^2/2\varepsilon^2}$ with $\varepsilon = 11°$. (*B*) An architecture that incorporates neurons that are insensitive to the direction of motion of the stimulus as well as those that are sensitive to the direction.

The absence of phase shifts in the experimentally observed cross-correlations (6, 7) indicates that $J_{\mathbf{RR}'}$ is excitatory. Furthermore, experimental evidence (4, 6) and computational considerations suggest that $J_{\mathbf{RR}'}$ is a rapidly decreasing function of $\Delta\theta_0$. The rate of decrease depends on the form of $F(\theta - \theta')$ (Eq. **12**). We consider first the possibility that the long-range connections represented by $F(\theta - \theta')$ are purely excitatory and occur only between neurons with similar orientation preferences; i.e., $F(\theta - \theta') \propto \delta(\theta - \theta')$. This hypothesis leads to an effective interaction whose dependence on $\Delta\theta_0$ is roughly twice the width of the neuronal tuning curve (Fig. 1*A*). A sharper dependence of $J_{\mathbf{RR}'}$ on $\Delta\theta_0$ requires the use of inhibitory as well as excitatory long-range connections. A simple form of such connectivity, shown in Fig. 2*A*, leads to $J_{\mathbf{RR}'} = (W_L/N)e^{-(\Delta\theta_0)^2/2\varepsilon^2}$, where ε determines the angular range of the effective interaction.

Directional Selectivity. We have considered so far only neurons that are sensitive to one direction of motion of the stimulus (Fig. 1*A*). Stimulating two clusters of neurons with co-linear bars moving in opposite directions—i.e., $\Delta\theta_0 = 180°$—will not generate coherence between the activity of neurons in the two clusters.

It is known from experiment that even neurons that are not selective to the direction of motion exhibit oscillatory output in response to a stimulus moving either forward or backward (6, 7). Yet the output of two such neurons remains uncorrelated when bars moving in opposite direction pass through their respective, receptive fields (6, 7). These observations can be accounted for within the model by incorporating neurons that are insensitive to the direction of motion of the stimulus (Fig. 2*B*). The short-range connections will not depend on the directional properties of the neurons. However, the long-range connections will occur predominantly between cells that are directionally selective and that have

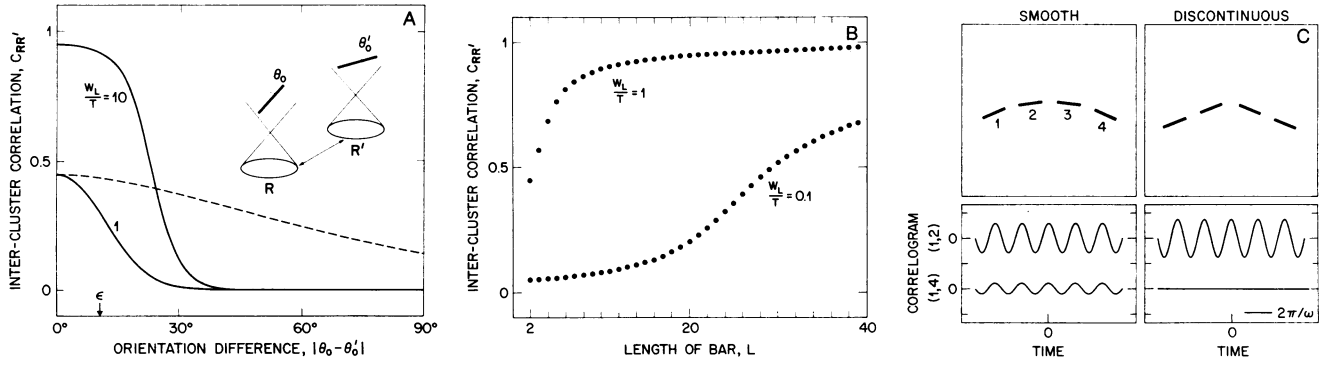

FIG. 3. Examples of the correlation between the average phases of two spatially separated clusters. (*A*) Correlation as a function of the difference in orientation of two moving, short bars. The solid lines correspond to an effective interaction that uses the connectivity shown in Fig. 2*A* while the dashed line assumes that only cells with identical orientation preference are connected. (*B*) Enhancement in the correlation between two clusters that are stimulated by a long bar as opposed to two co-linear short bars. The length of the bar is expressed as the number of receptive fields that it spans. (*C*) Segmentation of four oriented bars that span several receptive fields. The bars are of equal length and spacing and are arranged to subtend the same total angle ($W_L/T = 7$). For bars arranged as a smoothly varying stimulus, pair-wise correlations between adjacent clusters are equal with $C_{12} = C_{23} = C_{34} \simeq 0.6$ ($\Delta\theta_0 = 15°$). Neurons in all of the active clusters fire in partial synchrony and the end-to-end correlation is $C_{14} = (C_{12})^3 \simeq 0.2$. For bars arranged as discontinuous stimuli, pair-wise correlations between adjacent clusters are $C_{12} = C_{34} \simeq 0.8$ ($\Delta\theta_0 = 0°$) and $C_{23} \simeq 0$ ($\Delta\theta^0 = 45°$). The end-to-end correlation is $C_{14} \simeq 0$.

the *same* directional preference. As a consequence, only directionally sensitive neurons mediate the temporal coherence between different clusters. The output of the neurons in separate clusters will be coherent only when the two stimuli move in the same direction.

The spatial extent and features of the stimulus must be specified to evaluate the coherence between active clusters. We consider below several examples of extended stimuli and demonstrate the dependence of the coherence, $C_{RR'}$ (Eq. **11**), on global features of the stimulus. For each example we use the form of $F(\theta - \theta')$ shown in Fig. 2*A*, with ε chosen so that the half-width at half-maximum of $J_{RR'}$ is half that of the tuning curve.

Stimulation by Two Short Bars. The simplest example of long-range coherence involves two clusters that are stimulated by separate, short bars whose length spans the individual receptive fields (Fig. 3*A*, solid lines). The correlation of the average phases of the two clusters depends on the *relative* orientation of the bars through $J_{RR'}$. Note that the choice $F(\theta - \theta') \propto \delta(\theta - \theta_0)$ results in a relatively weak dependence of $C_{RR'}$ on $\Delta\theta_0$ (Fig. 3A, dashed line).

Short Versus Long Bars. The coherence between clusters can be enhanced when several receptive fields, as opposed to just two fields, are stimulated by bars moving with the same orientation. The enhancement depends on the magnitude of W_L/T and is most pronounced when this ratio is smaller than unity (Fig. 3*B*). The experimental evidence (6) is consistent with $W_L/T \lesssim 1$.

Extended Curved Objects. The curvature of stimuli that span several receptive fields can be used to segment a stimulus into separate objects. We illustrate this by considering the coherence between clusters in the presence of four, long bars with orientations that vary in space (Fig. 3*C*). In the case of a smooth variation there is a substantial correlation between the output of neurons in all pairs of clusters, including those at the end of the object. In contrast, with a discontinuous variation in orientation the coherent activity of the neurons is segmented into two groups.

DISCUSSION

Our results suggest that the experimental evidence for coherent oscillations in the cat visual cortex (4–7) has important implications regarding the underlying pattern of neuronal connectivity. (*i*) The effective interaction between the phases of the neuronal output depends on the level of activity in both the pre- and the postsynaptic cell. (*ii*) The connections formed by cells with overlapping receptive fields are significantly stronger than those between cells with nonoverlapping fields. (*iii*) Connections between cells with nonoverlapping receptive fields have a strong dependence on their respective orientational and directional preference.

In our model, we assumed that cells with substantially overlapping receptive fields form connections that do not depend strongly on the orientation preference of the pre- and postsynaptic cell. This choice allows proximal stimuli with disparate features to be linked as a single object. However, the experimental evidence regarding this issue is unclear (18).

The form of the interaction between the phases of the pre- and the postsynaptic neurons (Eq. **3**) is suggestive of a fast, Hebb-like modification of the strength of synaptic connection (2). However, the couplings between the phases of the neuronal oscillations will depend on the level of activity of the neurons even when the underlying synapses have a fixed strength. Whether this can account for the required dependence on the activity of the pre- and postsynaptic cells is an important issue.

The absence of phase shifts between the output of coherently active neurons resulted from the use of predominantly excitatory connections that did not contain time delays. However, the connections between cortical neurons with different receptive fields are mediated by axons with slow propagation speeds (9). The delays induced by these connections may be substantial. A preliminary analysis, similar to that in ref. 11, indicates that no phase shifts occur between the output of neurons in different clusters provided that the delay time is shorter than $\pi/2\omega$.

The presence of noise plays a vital role in controlling the coherence throughout the network. This is particularly crucial for dephasing the output of only weakly interacting clusters. Random variation in the driving frequency of each neuron [$\omega(\mathbf{r})$; Eq. **2**] is an additional, potential source of noise. Networks of coupled oscillators with a distribution of driving frequencies will remain coherent active provided that the width of this distribution is small relative to the strength of the interactions within a cluster (10); i.e., $|\delta\omega| \lesssim 1/\tau_S$ (Eq. **9**). In general, the coherence between different clusters can also be modulated by a variation of the driving frequency with some property of the stimulus. Systematic variation of the frequency with the velocity of visual stimuli is observed (4).

The role of cortical connections in maintaining phase coherence between neurons has been the topic of much

recent investigation (12–17). The modulation of the coherence of neuronal activity by orientation-coded stimuli has been studied by numerical simulations of circuits with relatively complex neuronal architectures and dynamics (12, 14, 15). Our phenomenological model of phase oscillators greatly simplifies the dynamics. It allowed a comprehensive, analytical study of the temporal and spatial coherence in terms of few parameters, e.g., the scales of short-range and long-range connection strength and the level of noise. This analysis provides explicit relations between the underlying neuronal connectivity and the computational capability of the network to segment extended stimuli.

APPENDIX

The equations for the noisy component of the phase of each neuron that incorporate our assumptions about the form of the connectivity are

$$\tau_0\dot{\phi}_{\mathbf{R}}(\theta, t) = \eta_{\mathbf{R}}(\theta, t) - (W_S/N)\sum_{\theta'} V_{\mathbf{R}}(\theta)V_{\mathbf{R}}(\theta')\sin(\phi_{\mathbf{R}}(\theta, t) - \phi_{\mathbf{R}}(\theta', t)) - (W_L/N^2)\sum_{\mathbf{R}'\neq\mathbf{R}}\sum_{\theta'} V_{\mathbf{R}}(\theta)F(\theta - \theta')V_{\mathbf{R}'}(\theta')\sin(\phi_{\mathbf{R}}(\theta, t) - \phi_{\mathbf{R}'}(\theta', t)). \quad [\mathbf{A1}]$$

The term $\eta_{\mathbf{R}}(\theta, t)$ represents white noise with a variance $2T\tau_0\delta(t - t')\delta_{\mathbf{R}\mathbf{R}'}\delta_{\theta\theta'}$. The sum over θ' includes all of the active neurons in a cluster. The sum over $\mathbf{R}'$ includes *only* clusters that are activated by the stimulus. The analysis of Eq. **A1** is performed in two stages. Terms that are of order unity describe the coherence of the activity *within* the clusters and do not involve the interactions between clusters. They are analyzed using mean-field theory, exact in the limit of large N; see Eq. **A2** below. The relationship *between* the phases of different clusters is described by terms that are of order $1/N$; see Eq. **A4** below.

The *intracluster* equations reduce to

$$\tau_0\dot{\phi}(\theta, t) = \eta(\theta, t) - W_S M\, V(\theta)\sin(\phi(\theta, t) - \psi), \quad [\mathbf{A2}]$$

where the coordinate of the cluster has been suppressed and the orientation of the stimulus is taken to be $\theta_0 = 0°$. The parameter M is determined self-consistently by

$$M = \int_0^{2\pi} (d\theta/\sigma)V(\theta)m(\theta), \quad [\mathbf{A3}]$$

where $m(\theta)$ is the *local order parameter* that characterizes the temporal coherence of the neurons with orientational preference θ. Both $m(\theta)$ and the phase ψ, which corresponds to the *mean* phase of the whole cluster, are defined by

$$m(\theta)e^{i\psi} = \langle e^{i\phi(\theta,t)}\rangle_\eta. \quad [\mathbf{A4}]$$

The phase ψ fluctuates on time scales of order $N\tau_0$ and does not affect the intracluster correlations on shorter time scales. Evaluating Eq. **A4** yields $m(\theta) = \mathbf{H}(W_S M V(\theta)/T)$, where $\mathbf{H}(x) = \mathbf{I}_1(x)/\mathbf{I}_0(x)$ is the ratio of modified Bessel functions. Substituting this result into Eq. **A3** yields a self-consistent equation for M. For T greater than $T_C = (W_S/2)\int_0^{2\pi} (d\theta/\sigma)V^2(\theta)$, the only solution is $M = 0$. For $V(\theta)$ of the form shown in Fig. 1*A*, $T_C \simeq 0.5\ W_S$. Below T_C, M is greater than zero. Using Eq. **A2** the correlation functions $C(\theta, \theta', \tau) = \langle\cos(\phi(\theta, t) - \phi(\theta', t + \tau))\rangle_\eta$ were evaluated. Their long-time limit is $m(\theta)m(\theta') = (C(\theta)C(\theta'))^{1/2}$ (Fig. 1*C* and Eq. **10**). The time dependence of the autocorrelation function is approximately $C(\theta, \tau) \simeq m^2(\theta) + (1 - m^2(\theta))e^{-\tau/\tau_S}$ with τ_S given by Eq. **9** (Fig. 1*B*).

The *intercluster* phase equations are found by summing Eq. **A1** over the internal coordinates of the clusters, θ and θ'; i.e.,

$$\tau_0\dot{\psi}_{\mathbf{R}}(t) = \eta_{\mathbf{R}}(t) - \sum_{\mathbf{R}'\neq\mathbf{R}} J_{\mathbf{R}\mathbf{R}'}\sin(\psi_{\mathbf{R}}(t) - \psi_{\mathbf{R}'}(t)), \quad [\mathbf{A5}]$$

where $\psi_{\mathbf{R}}$ is the average phase of the **R**th cluster, $\langle\eta_{\mathbf{R}}(t)\eta_{\mathbf{R}'}(t')\rangle = (2T/N)\delta_{\mathbf{R}\mathbf{R}'}\delta(t - t')$, and $J_{\mathbf{R}\mathbf{R}'}$ is given by Eq. **12**. The $\psi_{\mathbf{R}}$ vary on time scales of order $N\tau_0$. The equal-time correlation function between neurons in different clusters is given by Eq. **11** with $C_{\mathbf{R}\mathbf{R}'} \equiv \langle\cos(\psi_{\mathbf{R}}(t) - \psi_{\mathbf{R}'}(t))\rangle_\eta$. The function $C_{\mathbf{R}\mathbf{R}'}$ was calculated analytically for a few simple cases. For two, short bars at **R** and **R'**, Eq. **A5** reduces to a single equation for the phase difference $\psi_{\mathbf{R}} - \psi_{\mathbf{R}'}$. This yields $C_{\mathbf{R}\mathbf{R}'} = \mathbf{H}(NJ_{\mathbf{R}\mathbf{R}'}/T)$ (Fig. 3*A*). For the case of a long, straight bar spanning L receptive fields (Fig. 3*B*), there is a set of L fully connected phase oscillators with a constant coupling $J_{\mathbf{R}\mathbf{R}'}$ for $\Delta\theta_0 = 0°$. For the example of the smooth, curved object (Fig. 3*C*), the pair-wise interactions between nonadjacent clusters are negligible due to their orientation difference. This results in a linear chain of coupled oscillators.

We thank T. H. Bullock, F. H. C. Crick, C. M. Gray, P. Konig, C. v. d. Malsburg, and M. Stryker for stimulating discussions. This work was supported, in part, by the Fund for Basic Research administered by the Israeli Academy of Arts and Sciences and by the U.S.–Israel Binational Science Foundation.

1. von der Malsburg, C. & Schneider, W. (1986) *Biol. Cybern.* **54,** 29–40.
2. Gray, C. M., Konig, P., Engel, A. K. & Singer, W. (1990) in *Synergetics of Cognition*, eds. Haken, H. & Stadler, M. (Springer-Verlag, New York), pp. 82–98.
3. Crick, F. H. C. & Koch, C. (1990) *Semin. Neurosci.*, in press.
4. Eckhorn, R., Bauer, R., Jordan, W., Brosch, M., Kruse, W., Munk, M. & Reitboeck, R. J. (1988) *Biol. Cybern.* **60,** 121–130.
5. Gray, C. M. & Singer, W. (1989) *Proc. Natl. Acad. Sci. USA* **86,** 1698–1702.
6. Gray, C. M., Konig, P., Engel, A. K. & Singer, W. (1989) *Nature (London)* **338,** 334–337.
7. Engel, A. K., Konig, P., Gray, C. M. & Singer, W. (1990) *Eur. J. Neurosci.* **2,** 588–606.
8. Orban, G. A. (1984) *Neuronal Operations in the Visual Cortex* (Springer-Verlag, New York).
9. Martin, K. A. C. (1984) in *Cerebral Cortex*, eds. Jones, E. G. & Peters, A. (Plenum, New York), Vol. 3, pp. 241–284.
10. Kuramoto, Y. (1984) *Chemical Oscillations, Waves, and Turbulence* (Springer, New York).
11. Schuster, H. G. & Wagner, P. (1989) *Prog. Theor. Phys.* **81,** 939–945.
12. Sporns, O., Gally, J. A., Reeke, G. N. & Edelman, G. M. (1989) *Proc. Natl. Acad. Sci. USA* **86,** 7265–7269.
13. Kammen, D. M., Holmes, P. J. & Koch, C. (1989) in *Models of Brain Function*, ed. Cotterill, R. M. J. (Cambridge Univ. Press, Cambridge, U.K.), pp. 273–284.
14. Eckhorn, R., Reitboeck, R. J., Dicke, P., Arndt, M. & Kruse, W. (1990) in *Parallel Processing in Neural Systems and Computers*, eds. Eckmiller, R., Hartmann, E. & Hauske, G. (Elsevier, Amsterdam), pp. 101–104.
15. Schillen, T. B. & Konig, P. (1990) in *Parallel Processing in Neural Systems and Computers*, eds. Eckmiller, R., Hartmann, E. & Hauske, G. (Elsevier, Amsterdam), pp. 139–142.
16. Schuster, H. G. & Wagner, P. (1990) in *Parallel Processing in Neural Systems and Computers*, eds. Eckmiller, R., Hartmann, E. & Hauske, G. (Elsevier, Amsterdam), pp. 143–146.
17. Wilson, M. A. & Bower, J. A. (1990) in *Advances in Neural Network Information Processing Systems 2*, ed. Touretzky, D. (Morgan Kaufmann, San Mateo, CA), pp. 84–91.
18. Engel, A. K., Konig, P., Gray, C. M. & Singer, W. (1990) in *Parallel Processing in Neural Systems and Computers*, eds. Eckmiller, R., Hartmann, E. & Hauske, G. (Elsevier, Amsterdam), pp. 105–108.